miR-766-3p suppressed tumorigenesis, epithelial-mesenchymal transition, and metastasis by targeting BCL9L via β -catenin signaling pathway in osteosarcoma cells

Sheng Zhang
Jiangsu Province Hospital and Nanjing Medical University First Affiliated Hospital
Hongtao Chen
Jiangsu Province Hospital and Nanjing Medical University First Affiliated Hospital
Wanshun Liu
Jiangsu Province Hospital and Nanjing Medical University First Affiliated Hospital
Le Fang
Jiangsu Province Hospital and Nanjing Medical University First Affiliated Hospital
Zhanyang Qian
Southeast University Zhongda Hospital
Renyi Kong
Jiangsu Province Hospital and Nanjing Medical University First Affiliated Hospital
Qi Zhang
Nanjing Medical University Second Affiliated Hospital
Juming Li
Jiangsu Province Hospital and Nanjing Medical University First Affiliated Hospital
Xiaojian Cao (xiaojiancao001@163.com)
Jiangsu Province Hospital and Nanjing Medical University First Affiliated Hospital

Research

Keywords: Osteosarcoma, miR-766-3p, BCL9L, β-Catenin, EMT, Metastasis

Posted Date: August 20th, 2020

DOI: https://doi.org/10.21203/rs.3.rs-61546/v1

Abstract

Background

Emerging evidence has indicated that abnormal microRNAs (miRNAs) play critical roles in carcinogenesis and progression of osteosarcoma (OS). The aim of this study was to clarify the relationship between miR-766-3p expression and osteosarcoma development and to explore its potential mechanism.

Methods

miR-766-3p was the most downregulated miRNA by analyzing GSE65071 from the GEO database. RT-PCR and western blot was performed to determine miR-766-3p expression and its specific target gene in human OS samples and cell lines. CCK-8 proliferation, colony formation, EdU, wound-healing, and transwell assays were used respectively to evaluate the influences of miR-766-3p depletion or ectopic expression on OS proliferation, migration and invasion in vitro. And a mouse tumorigenicity model was conducted to investigate effects of miR-766-3p in vivo. Moreover, we identified directly interactions between miR-766-3p and its specific target gene using luciferase reporter assays.

Results

miR-766-3p expression was overexpressed in OS tissues and cell lines, and ectopic miR-766-3p expression repressed the malignant level of OS, including cell proliferation, migration, invasion and epithelial to mesenchymal transition (EMT) in vitro and in vivo. B-Cell Lymphoma 9-Like Protein (BCL9L) was negatively correlated with miR-766-3p expression in human OS tissue, and was validated as a downstream target of miR-766-3p by the luciferase reporter assay and Western blotting. Rescue experiment indicated that BCL9L could restore the effects of miR-766-3p on OS migration and invasion. The β-Catenin signaling pathway was demonstrated as being implicated in the miR-766-3p/BCL9L axis.

Conclusions

In conclusion, miR-766-3p is a negative regulator of BCL9L and a risk factor for tumor metastasis in OS progression.

Introduction

Osteosarcoma (OS), a primary high-grade malignant bone neoplasm arising from mesenchymal cells, has high mortality worldwide [1]. In recent years, regardless of the continuous development of treatments including chemotherapy techniques and various surgical methods, the 5-year survival rate of osteosarcoma is still < 70% [2, 3]. And it has a high potential for distant metastasis, particularly lung metastasis, and the 5-year survival rate of OS patients with lung metastasis is less than 30% [4, 5].

Therefore, in order to develop new potent therapeutic strategies, the underlying mechanism of OS metastasis must be elucidated.

During the initiation of metastasis process, epithelial–mesenchymal transition (EMT) plays a crucial role. EMT is a reversible phenotypic change in which polar epithelial cells lose epithelial characteristics and acquire properties of mesenchymal cells, which may help explain tumorigenesis and metastasis of OS [6–8]. Therefore, inhibition of EMT progression may be a potentially effective method for the treatment of OS.

MicroRNAs (miRNAs), a kind of endogenous small noncoding RNAs with a length of 22–28 nucleotides, negatively regulate target genes by binding to the 3'-untranslated regions (3'-UTRs) of the target mRNAs and degrading or translational inhibiting them [9, 10]. And accumulating evidence demonstrates that miRNAs act as the vital role of miRNA in the occurrence and development of various tumors by multiple signal pathways [11, 12]. miRNAs which may regulate cell proliferation, EMT, and metastasis are also identified important in the development of OS [13–15]. As a tumor-suppressing miRNA, miR-766-3p, which was reported to frequently downregulated in several types of cancer, was remarkably correlated with poor clinical outcomes [16, 17]. Nevertheless, to date, there have been no detailed investigations into the functions of miR-766-3p in OS, and the role of miR-766-3p is far from fully understood.

Expression levels of miR-766-3p assessed in hepatocellular carcinoma tissues and cell lines is lower compared to control samples, and was significantly correlated with tumor size, TNM stage, metastasis, and a poor prognosis of hepatocellular carcinoma by targeting Wnt family member 3A, metastasis-associated protein 3 and fos-related antigen 2 [18–20]. Furthermore, miR-766–3p functioned as a tumor-suppressor gene, which suppressed renal cancer cell-cycle progression by regulating the amplification of SF2 and additional downstream signaling pathways, and markedly correlated with a prognosis of renal cell carcinoma [21]. However, as we know, the exact value of miR-766-3p in osteosarcoma growth and metastasis is still unknown.

B-Cell Lymphoma 9-Like Protein (BCL9L), a second component of the vertebrate BCL9 family, is identified as cofactor of canonical Wnt signaling in mammalian cells and induces epithelial-mesenchymal transitions [22–24]. It has reported that BCL9L promotes early phases of intestinal tumor progression in humans by regulating the switch between the adhesive and transcriptional functions of β-catenin. Moreover, BCL9L is demonstrated to enhance β-catenin–mediated transcription and increase the proliferation as well as the metastatic potential of breast and colon cancer cells. However, studies revealing the role of BCL9L in osteosarcoma are rarely reported, and the relationship between the miR-766-3p–BCL9L axis and the Wnt signaling pathway involved in OS still remains to be investigated in depth.

In our study, it was found that miR-766-3p was significantly decreased in in OS cell lines and tumors and promoted, EMT and. We demonstrated that the overexpression of miR-766-3p suppressed EMT, proliferation and metastasis in OS by downregulating the expression of BCL9L via the β-catenin/TCF-4 signaling pathway.

Methods

Tissue samples

This study was approved by the Ethics Committee of The First Affiliated Hospital of Nanjing Medical University, and all experiments were conducted in accordance with the approved guidelines and regulations, and all the subjects signed the written informed consent. 60 pairs of osteosarcomas and adjacent normal tissue were collected from patients undergoing biopsy before the chemotherapy at the orthopedics department. Biopsy samples were obtained and subsequently frozen in liquid nitrogen. The clinical and demographic information of all patients is shown in Table 1.

Cell culture

All human OS cell lines (Saos-2, MG63, 143B, HOS, and U2OS) and the normal human fetal cell osteoblasts (hFOB1.19) were from the American Type Culture Collection (Manassas, VA, USA). And these cells were maintained in DMEM/F12 medium (Life Technologies, Grand Island, NY) supplemented with fetal bovine serum (FBS, 10%, Gibco, Grand Island, NY) and 1% penicillin/streptomycin (Gibco, Carlsbad, CA).

Establishment of stable transfected cell lines

Synthesis of lentiviruses pLV-hsa-miR-766-3p-pre-microRNA vector (miR-766-3p mimics), pLV-hsa-miR-766-3p-sponge inhibitor vector (miR-624-5p inhibitor), and vector containing the BCL9L DNA sequence (BCL9L) was authorized to GenePharma (Shanghai, China). Osteosarcoma cells transfection was performed in accordance with the manufacturer's protocol of Lipofectamine2000 (Invitrogen, CA, USA).

Quantitative Real-time quantitative polymerase chain reaction (qRT-PCR)

Total RNA from tissues and cells with Trizol (Invitrogen, USA) was extracted from the pulverized samples stored at liquid nitrogen, and was resuspended in DEPC-treated H2O. The concentration and purity of total RNA were confirmed at 260 nm. Reverse transcription (RT) was undertaken using the Goldenstar^{TM} RT6 cDNA Synthesis Kit (Beijing TsingKe Biotech Co. Ltd., China) according to the manufacturer's protocol. SYBR Green Master (TsingKe, Beijing, China) was for the quantitative PCR measure. The expression level of U6 or GAPDH served as the endogenous control. The primers for BCL9L, GAPDH, miR-624-5p, and U6 were obtained from TsingKe (Beijing, China). The sequences of the primers are shown in Supplementary table S1.

Migration assay

Cell migration assay was carried out using Transwell migration and Wound-healing assay. Transwell chambers (8-uM pore size; Costar, NY, USA) were used in the migration assay. In Brief, the Transwell co-culture assay was performed using the 12-well Transwell plates (Corning, MA, USA). 24 h later, cells that had passed through the Transwell membrane were fixed with paraformaldehyde, stained with crystal

violet and subsequently photographed in three random microscopic views. And the cells were counted and photographed under an optical microscope (Nikon, Tokyo, Japan). For wound-healing assay, OS cells were seeded in six-well plates and grown until 80–90% confluence overnight, and were scratched by a sterile 200μL pipette tip. The wound closure was observed at 0 and 24 h, and imaging performed under a microscope.

Invasion assay

To assess the cell invasive ability, Transwell invasion assays were performed. For Matrigel invasion assays, cells were seeded on the upper surface of membranes coated with Matrigel matrix (Millipore, USA). Following incubation for 24 h, cells invading across the Transwell membrane were fixed with 4% paraformaldehyde and stained with 0.4% crystal violet for 20 min. The stained cells were counted and photographed under a light microscope.

Cell counting Kit-8 assay (CCK-8) and colony formation assay

The transfected cells were plated in 96-well plates (5×10^3 cells with 100 μL/well) and cultured for 24, 48, 72, 96, and 120 h. Cell Proliferative rate was examined by the Cell Counting Kit-8 (CCK-8, Dojindo, Japan) following the manufacturer's instructions. The colony formation experiment was conducted by staining cell lines with crystal violet and counting the number of effective clones after culturing for 14 days.

5-ethynyl-2-deoxyuridine (EdU) incorporation assay

The 5-ethynyl-2-deoxyuridine (EdU) incorporation analysis was conducted according to the manufacturer's protocol of a kFluor 555 Click-iT EdU Imaging Kit (KeyGEN, Nanjing, China). And the images were captured by fluorescent microscope (Carl Zeiss, Germany).

Immunofluorescence analysis

Transfected cells were fixed with 4% paraformaldehyde for 10 min, and permeabilized with 0.3% Triton X-100 for 15 min. Then, the cells were immunofluorescence stained with the primary antibodies to β-catenin (Abcam, MA, USA), fluorescein-conjugated secondary antibody, and then with DAPI. Images were collected by fluorescence microscope (Carl Zeiss, Germany).

Luciferase reporter assay

We obtained possible miRNA-766-3p-binding sites from the TargetScan (http://targetscan.org) database. The synthesis of wild-type BCL9L (WT-BCL9L-3'-UTR) and mutant BCL9L (MUT-BCL9L-3'-UTR) were conducted by GenePharma (Shanghai, China). Cells overexpressing miR-766-3p or its control were compared with cells transfected with WT-BCL9L-3'-UTR and MUT-BCL9L-3'-UTR. Cells were acquired 48 h after transfection, and firefly luciferase activity was measured by the Dual-Luciferase Assay System (Promega, Madison, WI, USA), and normalized with Renilla luciferase.

Western blotting

After protein extraction, and the protein concentration was determined using BCA Protein Quantification Kit (Thermo, USA). Proteins were then subjected to 10% SDS-PAGE and transferred to polyvinylidene difluoride (PVDF) membranes (Bio-Rad, Hercules, CA, USA). Next, the membranes were blocked in 5% skim milk and incubated with primary antibodies (1:1000) at 4°C overnight. We used a panel of antibodies to detect these proteins, including Rabbit anti-BCL9L, GAPDH, N-cadherin, E-cadherin, vimentin, β-catenin, TCF-1, Cyclin D1 and Axin2 antibodies (Abcam, Cambridge, UK). And the membrane was washed with PBST followed by incubation with the secondary antibody (1:10000) for 1 h at room temperature. Reacting bands were achieved by ECL reagent (Shanghai Tianneng Technology Co., Ltd., Shanghai, China), and protein bands was semi-quantified using ImageJ.

Immunohistochemical staining

All tissue specimens were fixed in 4% paraformaldehyde overnight, embedded in paraffin, cut into 4-μm-thick sections and incubated with the primary antibody for BCL9L (Abcam, Cambridge, UK) overnight at 4 °C. Next, the sections were incubated with the secondary antibody for 1 h and stained using the developed diaminobenzidine (DAB) for 3 min. The staining results were measured by combining the percentage of positive staining and intensity of positively stained tumor cells.

Xenograft transplantation experiments

Animal studies were approved by the Animal Ethics Committee of Nanjing Medical University. Female BALB/c nude mice used for tumor growth assays were purchased from the Animal Model Institute of Nanjing University (Nanjing, China). The nude mice were randomly assigned into four groups, five in each group. OS cells (1×10^6cells), labeled with firefly luciferase, were subcutaneously injected into the nude mice. Tumor growth was observed every 3 days. Tumor size was expressed as tumor volume and calculated by the formula: $V = A \times B^2/2(mm^3)$, where “A” was the larger diameter and “B” was the smaller diameter. On day 35 post injection, the progression of xenograft growth was imaged with the IVIS200 imaging system (Caliper Life Sciences, Waltham, MA, USA).

Statistical analysis

All experiments were repeated at least three times, with average values expressed as means ± standard deviation (SD). The association of miR-766-3p expression with clinicopathological features was analyzed by the $\chi 2$ test. To compare significant differences between the two groups, comparisons were made by independent Student’s t-test. Statistical analysis of the differences in mRNA expression levels of miR-766-3p and BCL9L in paired tissues were analyzed by paired t-test. One-way or two-way ANOVA with Bonferroni post hoc test was tested for multivariate analysis. Pearson’s correlation analysis used for bivariate correlation. Statistical analyses were performed by SPSS, v. 20.0 (SPSS Inc., Chicago, IL, USA). $P< 0.05$ was considered as statistically significant.

Results

miR-766-3p expression was downregulated in OS cell lines and clinical tissues.

In order to investigate the expression level of miRNAs in OS tissues, we analyzed the data from the GEO database (GSE65071) using the R package limma. The volcano plot demonstrates the miRNA expression differences in normal and OS tissues (Fig. 1A). Totally, 70 miRNAs were downregulated (fold change > 2.0, FDR < 0.05) in OS tissues and the top 8 most significantly differentially expressed miRNAs are listed in Fig. 1B. According to the expression levels of miRNA, the up- and downregulated miRNAs was represented in a cluster heap map (Fig. 1C). We found the most down-regulated miRNA was miR-766-3p in these miRNAs. Thus, we tried to understand the molecular mechanism of the inhibition effect of miR-766-3p. As shown in Fig. 1D, miR-766-3p was significantly downregulated in OS tissues, compared with that of normal tissue. Then, real-time quantitative PCR was performed to demonstrate the miR-766-3p expression level in 60 paired OS tissues and adjacent normal tissues. Compared with peritumor tissues, miR-766-3p was significantly decreased in OS tissues (P< 0.001, Fig. 1E). In addition, it was proven that miR-766-3p was lowly expressed in patients with metastasis (P< 0.001, Fig. 1F).And expressing levels of miR-766-3p prominently decreased in OS cell lines, including Saos-2, HOS, 143B, U2OS, and MG-63, compared with in hFOB 1.19 cells (P< 0.001, Fig. 1G). And as shown in representative images of OS patients with or without lung metastasis (Supplementary Fig. S1), the red arrows indicated tumor foci or pulmonary metastatic nodules. In order to identify the clinical significance of miR-766-3p in OS, median expression level of miR-766-3p was defined as a cutoff value and the patients were divided into subgroups. In Table 1, the expression level of miR-766-3p was significantly negatively correlated with TNM stage, tumor size, and lung metastasis.

Downregulating miR-766-3p promoted OS cell migration and invasion in vitro.

Among these OS cell lines, 143B and U2OS cells were used to study further in vitro experiments. The transfection efficiency of miR-766-3p was verified lentiviruses by qRT-PCR. The results revealed that miR-766-3p was significantly overexpressed in the mimics group and constrained in the inhibitor group (U2OS, P< 0.001; 143B, P< 0.001; Fig. 2A). Western blot analysis demonstrated that miR-766-3p sh#1 and miR-766-3p sh#2 diminished E-cadherin levels and raised the metastasis related protein levels of N-cadherin and vimentin in U2OS and 143B cells (Fig. 2B). To explicate the effects of miR-766-3p on OS cell migration and invasion ability in vitro, we conducted migration and invasion assays. The wound-healing assay and Transwell migration assay showed that down-regulated expression of miR-766-3p could promote the migration of U2OS and 143B cells (U2OS, P< 0.001; 143B, P< 0.001; Fig. 2C-F). The Transwell invasion assay indicated that the knockdown of miR-766-3p significantly increased the number of invasive OS cells per field (U2OS, P< 0.001; 143B, P< 0.001; Fig. 2G, H). Besides, CCK-8, colony formation and EdU assays were detected the effect of miR-766-3p promotion on OS cell proliferation. As can be seen from Additional file 1: Figs. S2A, B, downregulating miR-766-3p revealed no significant difference in the first three days, but significantly promoted cell proliferation after five days, showing that miR-766-3p

has the potential as inhibitory factor in OS cell proliferation. The results of colony formation and Edu assays were consistent with the above result (Additional file 1: Figs. S2C-F).

Overexpression of miR-766-3p inhibited OS cell migration and invasion in vitro.

Western blot analysis revealed that E-cadherin levels was raised in the miR-766-3p mimic group, and the metastasis related protein levels of N-cadherin and vimentin was downregulated in U2OS and 143B cells (Fig. 3A).Transwell migration assays were performed and the results showed that miR-766-3p overexpression remarkably promoted the migration abilities of U2OS and 143B cells (U2OS, $P< 0.01$; 143B, $P< 0.01$; Fig. 3B, C), and the wound-healing assay were similar to those of the Transwell migration assay results (U2OS, $P< 0.001$; 143B, $P< 0.001$; Fig. 2D, E). Then, Transwell invasion assays were conducted to assess the effects of miR-766-3p on invasion. The results were consistent with those of the Transwell migration and wound-healing assays (U2OS, $P< 0.001$; 143B, $P< 0.001$; Fig. 2F, G). Moreover, the CCK-8, EdU and colony formation assays revealed that overexpression of miR-766-3p markedly decreased the proliferation of U2OS and 143B cells (Additional file 1: Figs. S2). Taken together, these data suggest that miR-766-3p mediates OS cells invasion, migration and proliferation processes.

BCL9L expression was upregulated in OS cell lines and tissues and was a target of miR-766-3p.

To further detect the underlying mechanism of miR-766-3p in the invasion, migration and proliferation of OS cells, Potential targets of miR-766-3p were predicted using TargetScan, miRDB and miRTarBase Tools (Additional file 1: Figs. S3). Among the candidate genes, we were specifically interested in BCL9L because it played essential tumor-promoting role in modulation of carcinogenesis and cancer development. The qRT-PCR and Western blotting were used to explore BCL9L expression in 60 paired OS tissues and adjacent tissues. PTPRB expression was significantly more in tumor tissues than the adjacent tissues ($P< 0.05$, Fig. 4A, B). These results were confirmed by immunohistochemistry assays (Fig. 4C). Further, we found that the expression level of BCL9L was negatively correlated with miR-766-3p in OS tissues with an R2 of 0.4751 (Fig. 4D). As demonstrated in Fig. 4E, *Kaplan-Meier* analysis revealed that patients with high expression of BCL9L had significantly poor survival than those with low expression ($P= 0.0031$). Furthermore, the mRNA of BCL9L was observed to be upregulated in OS cell lines, particularly in U2OS and 143B cells ($P < 0.001$, Fig. 4F). And western blotting results showed that U2OS and 143B cells contained the most amount of BCL9L protein compared to the other cell lines ($P < 0.001$, Fig. 4G). Besides, the median values of miR-766-3p and BCL9L mRNA levels were used as cutoff points to divide patients into “high” and “low” subgroups. Table 1 indicated that the expression level of BCL9L was positively related to tumor size, TNM stage, and lung metastasis. Next, we carried out-luciferase reporter assay analysis to confirm that miR-766-3p could directly targeted BCL9L. It revealed that miR-766-3p overexpression could significantly reduce the activity of luciferase in OS cells (Fig. 4H). As shown in Fig. 4I, quantitative RT-PCR analysis showed low mRNA expression of BCL9L in cells transfected with miR-766-3p mimics; in contrast, a markedly high BCL9L expression was investigated in cells with miR-766-3p inhibitor. What is more, Western blotting assays determined that miR-766-3p negatively regulated the

expression level of BCL9L (Fig. 4J). In summary, these results showed that BCL9Lwas a direct target of miR-766-3p.

Upregulating BCL9L abolished the effects of miR-766-3p mimics on OS migration and invasion.

In order to further confirm that miR-766-3p mediates OS cell migration and invasion by targeting BCL9L, we did a series of rescue experiments. First, OS cells were transfected with miR-766-3p mimics to realize miR-766-3p upregulation. Then, Western blotting revealed that E-cadherin expressions in 143B and U2OS cells were remarkably decreased by the overexpression of miR-766-3p, while BCL9L and the metastasis-related proteins (N-cadherin and vimentin) did a significant increase. Surprisingly, these influence of miR-766-3p mimics were evidently reversed by overexpressed BCL9L (Fig. 5A). Transwell migration assays were conducted and the results showed that BCL9L inhibited the protective influences of OS cell invasion resulting from miR-766-3p mimics (U2OS, $P< 0.001$; 143B, $P< 0.001$; Fig. 5B); the inhibitory effects of cell migration resulting from miR-766-3p mimics were reduced by BCL9L upregulation in the wound-healing assays (U2OS, $P< 0.001$; 143B, $P< 0.001$; Fig. 5C). As shown in Fig. 5D, the above results were also verified in Transwell invasion assays. Taken together, BCL9L was confirmed to be helpful in promoting OS cell migration and invasion caused by miR-766-3p

miR-766-3p regulated the β-catenin/TCF-1 signal pathway through BCL9L.

To demonstrate the underlying mechanism of how the miR-766-3p /BCL9L axis modulates OS cells migration and invasion, we performed Western blotting and immunofluorescence analysis. It has been reported that the Wnt/β-catenin signaling pathway is involved in cancer development. And previous studies revealed that it was a critical step in the tumorigenesis of various types of tumors, including the muscular and skeletal systems. So, whether miR-766-3p and BCL9L influenced OS invasion and migration through the Wnt/β-catenin pathway was the focus of our study. Western blotting assay indicated that miR-766-3p mimics in 143B and U2OS cells reduced BCL9L expression, as well as downregulated the levels of β-catenin, TCF-4, Cyclin D1 and Axin2, but the inhibiting effects were all remedied by upregulating BCL9L (Fig. 6A). What is more, the expression of β-catenin protein contained in the nuclei were negatively related with the miR-766-3p level and had a positive correlation with the expression level of BCL9L (Fig. 6B). Immunofluorescence analysis provided vigorous evidence that miR-766-3p mimics enhanced β-catenin import into the nuclei of 143B and U2OS cells and overexpressing BCL9L could abolish this effect (U2OS, $P< 0.001$; 143B, $P< 0.001$; Fig. 6C). Overall, these results indicate that the miR-766-3p/BCL9L axis regulates OS cell migration, invasion, and proliferation via the β-catenin/TCF-4 signal pathway.

miR-766-3p promoted xenograft tumor growth in vivo.

In order to detect the effects of miR-766-3p on tumor growth in vivo, 143B cells stably upregulated or U2OS cells with suppressed miR-766-3p were subcutaneously injected into nude mice. And we used cells transfected with miR-NC or sh-miR-NC to treat nude mice as negative controls. The xenograft tumor sizes were monitored every 2 days from 14 days after injection, and 4 weeks later the mice were euthanized.

Fig. 7A, B showed that knockdown of miR-766-3p accelerated the growth of OS cells ($P < 0.01$), and the tumor volume and weight were larger and heavier respectively ($P < 0.01$, Fig. 7C; $P < 0.01$, Fig. 7D). On the contrary, high expression of miR-766-3p remarkably suppressed tumor growth compared to controls ($P < 0.01$, Fig. 7E, F), and the tumor was smaller and lighter ($P < 0. 01$, Fig. 7G; $P < 0.01$, Fig. 7H). Then, to examine the expression level of BCL9L in xenografts, immunohistochemistry revealed that the expression level of BCL9L was enhanced by miR-766-3p inhibitor; in contrast, miR-766-3p mimics decreased BCL9L expression (Fig. 7I, J). Furthermore, the variation expression of BCL9L in xenografts was confirmed by Western blotting ($P < 0.01$, Fig. 7K; $P < 0.01$, Fig. 7L). Taken together, miR-766-3p plays a significant role in promoting proliferation of OS cells in vivo. As shown in the mechanism diagram, miR-766-3p and BCL9L played a crucial role in the occurrence and development of OS; additionally, miR-766-3p suppressed OS cell proliferation, EMT and metastasis via β-catenin/TCF-4 signal pathway, and directly targeted BCL9L (Fig. 8).

Discussion

As mentioned in the previous studies, osteosarcoma occurring predominantly in children and adolescents is the most frequent primary malignant bone sarcoma [1, 3, 4, 25]. Although previous studies have revealed that miRNAs have a significant influence on modulating cellular functions and biological processes of various tumors [9, 12, 26], Unfortunately, little is known about the mechanism underlying the pathogenesis of OS. Therefore, there is an urgent requirement to understand the mechanism of development and metastasis of OS and to identify novel therapies [5, 27, 28]. In this study, a series of experiments were conducted and the results indicated that miR-766-3p was downregulated in OS tissues and cell lines. Moreover, miR-766-3p was negatively correlated with malignancy of OS, and could be used as a novel target for OS treatment.

Emerging research has demonstrated that the abnormal miRNA expression plays key regulatory role in OS progression [29, 30], the underlying mechanisms of miR-766-3p in OS have not yet been detected. MiR-766-3p has recently been recognized as a tumor suppressor by inhibiting the Wnt pathway in several tumors. MiR-766-3p was lower in hepatocellular carcinoma and renal cell carcinoma specimens or cell lines than in normal group. Similarly, our findings via real-time quantitative PCR are consistent with those from previous studies [16, 19, 21]. In the current study, we first found that miR-766-3p was downregulated in clinical OS samples and cell lines, indicating that this RNAs may function as a tumor suppressor. And we performed a series of experiments in vitro, showing that miR-766-3p inhibited aggressive and invasion of OS cells.

EMT has long been linked to cancer malignant progression, tumor migration and metastasis [31, 32]. During this process, epithelial cancer cells acquire a mesenchymal phenotype, which was characterized by the loss of cell–cell adherent junctions, loss of cell polarity and actin cytoskeleton remodeling. And these central changes enhance migration, invasion of cancer cells and confer resistance to therapy [33-35]. In addition, other characteristics of the EMT phenotype is downregulation of epithelial markers (E-cadherin) and upregulation of mesenchymal markers (N-cadherin and Vimentin) [6, 7]. In our study,

overexpression of E-cadherin in cells was observed by an upregulated miR-766-3p level; however, when miR-766-3p was overexpressed, the levels of Vimentin and N-cadherin decreased. Consistent with our in vitro results, miR-766-3p suppressed the ability of OS cell metastasis, indicating that miR-766-3p acted as a risk factor in OS progression. Moreover, we demonstrated that BCL9L is one target genes of miR-766-3p. We first confirmed that miR-766-3p abolished BCL9L expression in OS cells both at the mRNA and protein levels, and miR-766-3p was negatively correlated with BCL9L expression in OS tissues. Then, the luciferase reporter assay showed that the luciferase activity of WT-BCL9L-3'-UTR but not MUT-BCL9L-3'-UTR was inhibited by miR-766-3p. Furthermore, BCL9L was downregulated in OS cells and recovery of its expression could reverse the effects of miR-624-5p.

BCL9L, a type of protein like B-Cell CLL/Lymphoma 9 (BCL9), is a second component of the vertebrate BCL9 family, and is usually regarded as cofactor of canonical Wnt signaling in mammalian cells and induces epithelial-mesenchymal transitions [36, 37]. BCL9L was shown to promote tumor progression of breast cancer [38], choriocarcinoma [39], pancreatic cancer [40], and colon cancer [22, 41, 42]. It was reported that higher expression of BCL9L predict lower survival rates in intestinal tumor patients and could be employed as an independent prognostic biomarker. Additionally, BCL9L was aberrantly elevated in 43% of colorectal tumors, and was required for enhanced β-catenin-TCF–mediated transcription in colorectal tumor cells. Here, our study findings validate that BCL9L is significantly upregulated among OS tissues, relative to the corresponding noncancerous tissues, indicating that BCL9L plays a promotable role in tumorigenesis and progression of OS.

Wnt signaling pathways regulate various processes that are essential for cancer progression, including tumor initiation, tumor growth, cell senescence, cell death, differentiation and metastasis [43, 44]. And β-catenin-dependent Wnt signaling pathways have crucial roles in the regulation of cancer cell above behaviors [45, 46]. Moreover, β-catenin functions as a transcriptional switch, which reduces the association of TLE with TCF/LEF , while recruiting various transcriptional cofactors including BCL9/BCL9L, Pygopus and histone acetyltransferases [36, 37, 47]. Considering that we further examined whether miR-766-3p inhibits the Wnt pathway via BCL9L. Overexpression of miR-766-3p decreased the levels of β-catenin, TCF, Cyclin D1 and Axin2, together with the downregulated BCL9L by Western blotting. On the contrary, downregulating miR-766-3p escalated levels of the above proteins. In addition, the application of siBCL9L or BCL9L markedly remedied the effects of miR-766-3p inhibitors or mimics on the Wnt signaling pathway. Immunofluorescence further showed that more β-catenin proteins were transported to the nuclei of OS cells while upregulating miR-766-3p or siBCL9L could abolish this effect.

Conclusions

In summary, we demonstrated the tumor-inhibiting role of miR-766-3p in osteosarcoma development and its underlying mechanism via BCL9L and the Wnt pathway. Our data reported that miR-766-3p had a suppressing role in OS progression. We demonstrated that miR-766-3p inhibited tumor progression both in vitro and in vivo. We further validated that miR-766-3p inhibited cell proliferation, migration, and EMT in OS cells through Wnt signaling activity by directly regulating BCL9L. The present study may provide

further insight into the development of osteosarcoma. Therefore, it is a reasonable inference that miR-766-3p/BCL9L signaling may provide valuable information for OS targeted therapy, which may be helpful to control the OS proliferation and metastasis, and even improve survival rate for the patients in the future.

Abbreviations

OS: Osteosarcoma; EMT: Epithelial-mesenchymal transition; IHC: Immunohistochemistry; BCL9L: B-Cell Lymphoma 9-Like Protein.

Declarations

Availability of data and materials

Most of the datasets supporting the conclusions of this article are included within this article and the additional files. The datasets used or analyzed during the current study are available on reasonable request.

Ethics approval and consent to participate

All animal procedures were performed under the guidelines of the institutional review board and the ethics committee of Nanjing Medical University. The study was approved by the Chinese Ethical Review Committee and signed informed consent was obtained from each patient.

Consent for publication

All the patients that involved in the study have given their consent to publish their individual data.

Competing interests

The authors declare no conflict of interest.

Funding

This study was supported by the National Natural Science Foundation of China (Grant nos. 81371968, 81672152, 81871773).

Authors' contributions

SZ performed the experiments, analyzed the data, and wrote the manuscript. HC, WL and LF conceived the study and revised the manuscript. ZQ, RK and QZ performed the experiments and analyzed the data.

JL and XC conceived, designed, and supervised the research. All authors read and approved the final manuscript. All authors declare that they have no conflict of interest. All authors approved the final version of the manuscript.

Acknowledgements

Not applicable.

References

1. Ottaviani G, Jaffe N. The epidemiology of osteosarcoma. Cancer Treat Res. 2009;152:3–13.
2. Isakoff MS, Bielack SS, Meltzer P, Gorlick R. Osteosarcoma: Current Treatment and a Collaborative Pathway to Success. J Clin Oncol. 2015;33(27):3029–35.
3. Kansara M, Teng MW, Smyth MJ, Thomas DM. Translational biology of osteosarcoma. Nat Rev Cancer. 2014;14(11):722–35.
4. Aljubran AH, Griffin A, Pintilie M, Blackstein M. Osteosarcoma in adolescents and adults: survival analysis with and without lung metastases. Ann Oncol. 2009;20(6):1136–41.
5. Luetke A, Meyers PA, Lewis I, Juergens H. Osteosarcoma treatment - where do we stand? A state of the art review. Cancer Treat Rev. 2014;40(4):523–32.
6. Kudo-Saito C, Shirako H, Takeuchi T, Kawakami Y. Cancer metastasis is accelerated through immunosuppression during Snail-induced EMT of cancer cells. Cancer Cell. 2009;15(3):195–206.
7. Brabletz T, Kalluri R, Nieto MA, Weinberg RA. EMT in cancer. Nature reviews Cancer. 2018;18(2):128–34.
8. De Craene B, Berx G. Regulatory networks defining EMT during cancer initiation and progression. Nature reviews Cancer. 2013;13(2).
9. I B-N CMP. B P, GA C. MicroRNAome genome: a treasure for cancer diagnosis and therapy. Cancer J Clin. 2014;64(5):311–36.
10. Rupaimoole R, Slack FJ. MicroRNA therapeutics: towards a new era for the management of cancer and other diseases. Nat Rev Drug Discov. 2017;16(3):203–22.
11. R G, G M, CM C. Targeting microRNAs in cancer: rationale, strategies and challenges. Nat Rev Drug Discov. 2010;9(10):775–89.
12. GA RR, G L-B C. AK S. miRNA Deregulation in Cancer Cells and the Tumor Microenvironment. Cancer discovery. 2016;6(3):235–46.
13. Y BS, MA W. T, G B, A F, M K, et al. Molecular mechanism of chemoresistance by miR-215 in osteosarcoma and colon cancer cells. Mol Cancer. 2010;9:96.
14. AL L, MJ S. MR E, A C. MicroRNA expression patterns and signalling pathways in the development and progression of childhood solid tumours. Mol Cancer. 2017;16(1):15.

15. K Z LL. J Z, Y W, H L, G F, et al. MiR-29b suppresses the proliferation and migration of osteosarcoma cells by targeting CDK6. Protein cell. 2016;7(6):434–44.
16. Z SLZL, W R Z. Y L, H C, et al. Serum exsomal miR-766-3p expression is associated with poor prognosis of esophageal squamous cell carcinoma. Cancer science. 2020.
17. Zhou N, Zhu X, Man L. LINC00963 Functions as an Oncogene in Bladder Cancer by Regulating the miR-766-3p/MTA1 Axis. Cancer Manag Res. 2020;12:3353–61.
18. Liu L, Qi X, Gui Y, Huo H, Yang X, Yang L. Overexpression of circ_0021093 circular RNA forecasts an unfavorable prognosis and facilitates cell progression by targeting the miR-766-3p/MTA3 pathway in hepatocellular carcinoma. Gene. 2019;714:143992.
19. You Y, Que K, Zhou Y, Zhang Z, Zhao X, Gong J, et al. MicroRNA-766-3p Inhibits Tumour Progression by Targeting Wnt3a in Hepatocellular Carcinoma. Mol Cells. 2018;41(9):830–41.
20. Li Z, Liu Y, Yan J, Zeng Q, Hu Y, Wang H, et al. Circular RNA hsa_circ_0056836 functions an oncogenic gene in hepatocellular carcinoma through modulating miR-766-3p/FOSL2 axis. Aging. 2020;12(3):2485–97.
21. Chen C, Xue S, Zhang J, Chen W, Gong D, Zheng J, et al. DNA-methylation-mediated repression of miR-766-3p promotes cell proliferation via targeting SF2 expression in renal cell carcinoma. Int J Cancer. 2017;141(9):1867–78.
22. FH B. M W, N Z, T G, Y D, J F, et al. BCL9-2 promotes early stages of intestinal tumor progression. Gastroenterology. 2011;141(4):1359–70, 70.e1-3.
23. M K, M K. WNT signaling pathway and stem cell signaling network. Clinical cancer research: an official journal of the American Association for Cancer Research. 2007;13(14):4042–5.
24. DM G, RA R. M M, MC H, A H, W C, et al. Loss of BCL9/9 l suppresses Wnt driven tumourigenesis in models that recapitulate human cancer. Nature communications. 2019;10(1):723.
25. Lindsey BA, Markel JE, Kleinerman ES. Osteosarcoma Overview. Rheumatol Ther. 2017;4(1):25–43.
26. RI SL. G. MicroRNA biogenesis pathways in cancer. Nature reviews Cancer. 2015;15(6):321–33.
27. DM G. L M, SA S. Germline and somatic genetics of osteosarcoma - connecting aetiology, biology and therapy. Nature reviews Endocrinology. 2017;13(8):480–91.
28. LC S, MR B, AL K, SG L, AG L, HY L, et al. Genome-Informed Targeted Therapy for Osteosarcoma. Cancer discovery. 2019;9(1):46–63.
29. Luo Y, Liu W, Tang P, Jiang D, Gu C, Huang Y, et al. miR-624-5p promoted tumorigenesis and metastasis by suppressing hippo signaling through targeting PTPRB in osteosarcoma cells. Journal of experimental clinical cancer research: CR. 2019;38(1):488.
30. Fellenberg J, Lehner B, Saehr H, Schenker A, Kunz P. Tumor Suppressor Function of miR-127-3p and miR-376a-3p in Osteosarcoma Cells. Cancers. 2019;11(12).
31. Mittal V. Epithelial Mesenchymal Transition in Tumor Metastasis. Annu Rev Pathol. 2018;13:395–412.

32. Thiery JP. Epithelial-mesenchymal transitions in tumour progression. Nature reviews Cancer. 2002;2(6):442–54.
33. Dongre A, Weinberg RA. New insights into the mechanisms of epithelial-mesenchymal transition and implications for cancer. Nat Rev Mol Cell Biol. 2019;20(2):69–84.
34. Lamouille S, Xu J, Derynck R. Molecular mechanisms of epithelial-mesenchymal transition. Nat Rev Mol Cell Biol. 2014;15(3):178–96.
35. Jolly MK, Somarelli JA, Sheth M, Biddle A, Tripathi SC, Armstrong AJ, et al. Hybrid epithelial/mesenchymal phenotypes promote metastasis and therapy resistance across carcinomas. Pharmacol Ther. 2019;194:161–84.
36. T N SATJTY. S O, Y O, et al. Role of a BCL9-related beta-catenin-binding protein, B9L, in tumorigenesis induced by aberrant activation of Wnt signaling. Cancer research. 2004;64(23):8496–501.
37. C C. P P, TD S, D Z, T V, G H, et al. A cytoplasmic role of Wnt/β-catenin transcriptional cofactors Bcl9, Bcl9l, and Pygopus in tooth enamel formation. Science signaling. 2017;10(465).
38. H T, T O SO. N T, I S, J H, et al. Immunohistochemical expression of the beta-catenin-interacting protein B9L is associated with histological high nuclear grade and immunohistochemical ErbB2/HER-2 expression in breast cancers. Cancer Sci. 2007;98(4):484–90.
39. K M, K T TJ. Y M, S A, T S, et al. Identification of a link between Wnt/β-catenin signalling and the cell fusion pathway. Nature communications. 2011;2:548.
40. C H. J P, L D, B K, K T. BCL9L expression in pancreatic neoplasia with a focus on SPN: a possible explanation for the enigma of the benign neoplasia. BMC Cancer. 2016;16:648.
41. de la Roche M, Worm J, Bienz M. The function of BCL9 in Wnt/beta-catenin signaling and colorectal cancer cells. BMC Cancer. 2008;8:199.
42. Deka J, Wiedemann N, Anderle P, Murphy-Seiler F, Bultinck J, Eyckerman S, et al. Bcl9/Bcl9l are critical for Wnt-mediated regulation of stem cell traits in colon epithelium and adenocarcinomas. Cancer Res. 2010;70(16):6619–28.
43. A K, W B. Wnt signalling and its impact on development and cancer. Nature reviews Cancer. 2008;8(5):387–98.
44. JN A, RT M. WNT signalling pathways as therapeutic targets in cancer. Nature reviews Cancer. 2013;13(1):11–26.
45. R N, H C. Wnt/β-Catenin Signaling, Disease, and Emerging Therapeutic Modalities. Cell. 2017;169(6):985–99.
46. MJ P, A E-B POIL, JJG MM. M, et al. Wnt-β-catenin signalling in liver development, health and disease. Nature reviews Gastroenterology hepatology. 2019;16(2):121–36.
47. Y T, D DG, C Y. M, F S, Y W, et al. KAT2A succinyltransferase activity-mediated 14-3-3ζ upregulation promotes β-catenin stabilization-dependent glycolysis and proliferation of pancreatic carcinoma cells. Cancer letters. 2020;469:1–10.

Tables

Table 1 Expression of miR-766-3p and BCL9L according to patients' clinical features

		miR-766-3p expression			BCL9L expression		
Characteristics	Total	High group	Low group	*P value*	High group	Low group	*P value*
Age(y)							
< 18	35	17	18	0.73	18	17	0.97
≥18	25	11	14		13	12	
Gender							
Female	28	15	13	0.45	14	15	0.61
Male	32	14	18		17	14	
Location							
Femur/Tibia	45	22	23	0.55	21	20	0.63
Elsewhere	15	6	9		11	8	
TNM stage							
I	27	14	13	0.02*	9	18	0.01*
II/III	33	8	25		22	11	
Tumor size (cm)							
< 5	31	17	14	0.032*	11	19	0.01*
≥5	29	8	21		21	9	
Lung metastasis							
Yes	26	4	22	0.005*	17	7	0.008*
No	34	17	17		13	23	

*P < 0.05(Chi-square test)

Figures

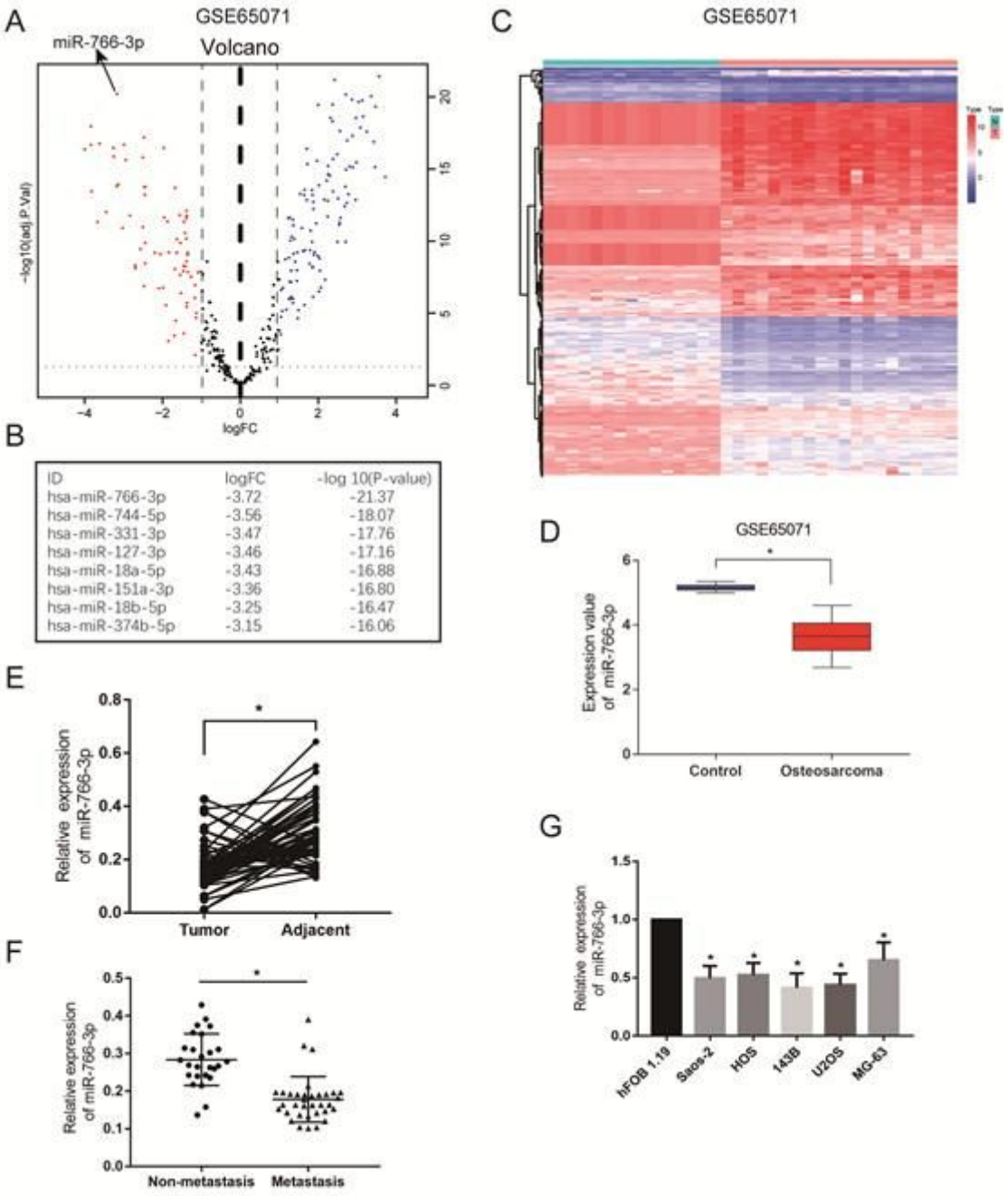

Figure 1

miR-766-3p is downregulated in osteosarcoma (OS) cell lines and clinical tissues. A. Volcano plot compared the differentially expressed miRNAs between OS and normal tissues from GSE65071. B. The top 8 downregulated miRNAs are listed. C. The cluster heap map showed the up-regulated and down-regulated microRNAs (miRNAs) in GSE65071. D–E. Expression of miR-766-3p was markedly downregulated in OS clinical tissues from GSE65071 and in-house cohort. F. miR-766-3p was notably downregulated in patients according to in-house cohort with metastasis. G. The relative expression of miR-766-3p was significantly decreased in OS cell lines (n= 4). Data are presented as the means ± SD. * P < 0.01.

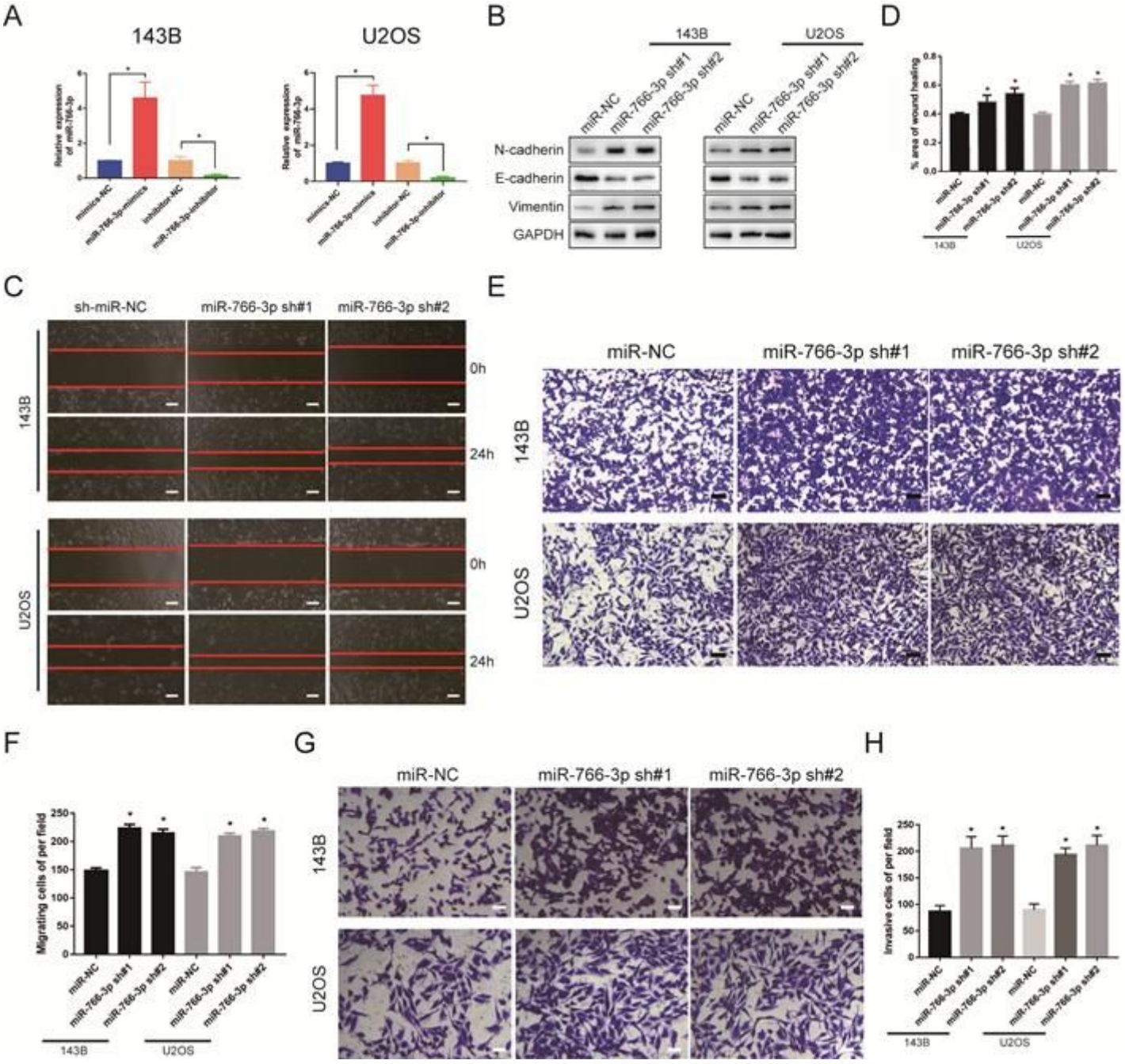

Figure 2

Downregulating miR-766-3p promoted OS cell EMT, migration and invasion in vitro. A. miR-766-3p lentiviruses were successfully transfected into 143B and U2OS cell lines (n = 3). B. miR-766-3p sh#1 and miR-624-5p sh#2 increased the expression level of metastasis-related proteins in 143B and U2OS (n = 3). C-F. The knockdown of miR-766-3p notably promoted the invasion and migration of 143B and U2OS cells (n = 4). G-H. The Transwell invasion assays indicated that the knockdown of miR-766-3p significantly increased the invasive ability of OS cells (n = 4). Data are presented as the means ± SD. * P < 0.01.

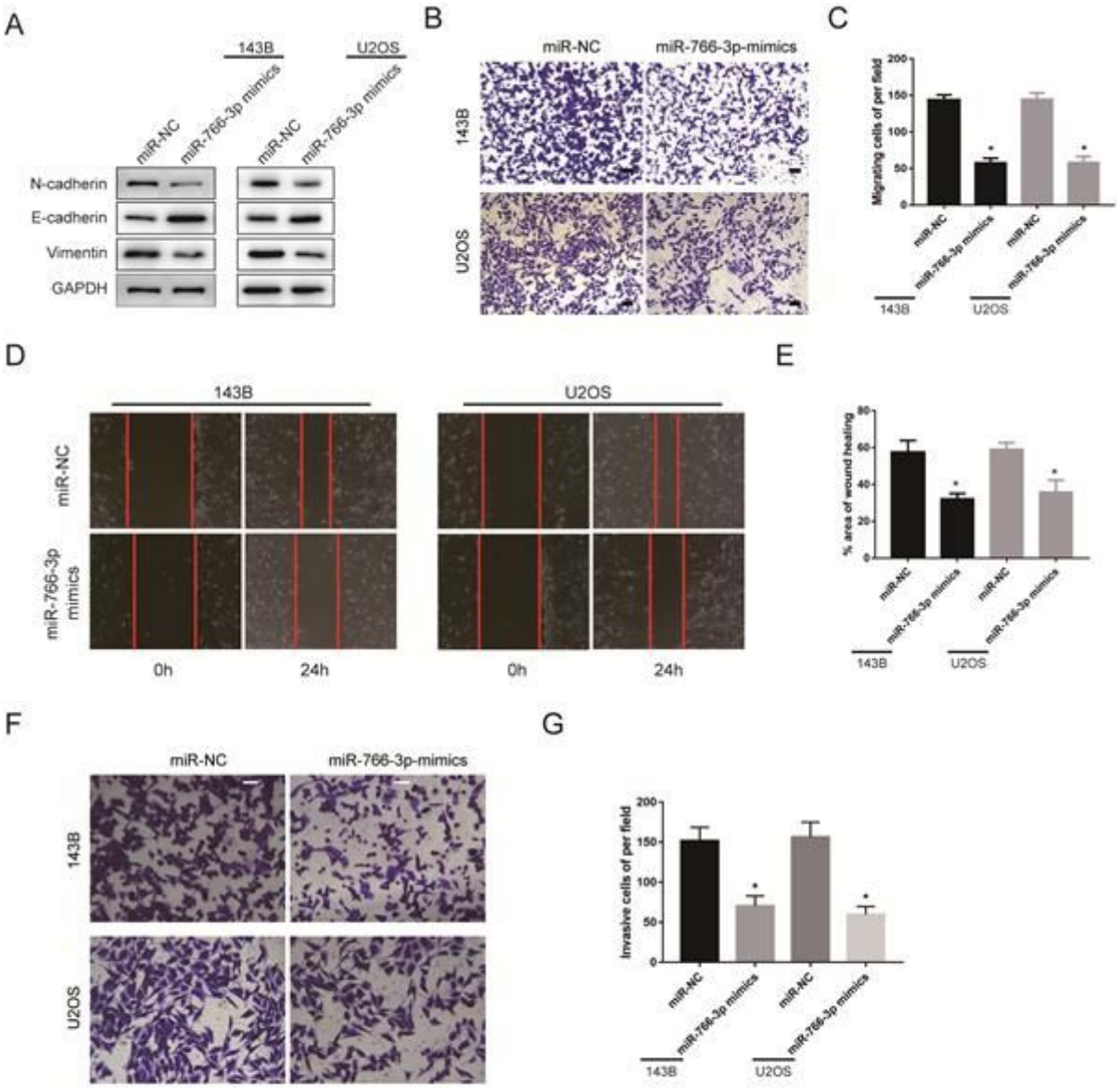

Figure 3

miR-766-3p suppressed OS cell EMT, migration and invasion in vitro. A. Western blotting demonstrated that miR-766-3p inhibited the EMT progression (n = 3). B-E. Upregulating miR-766-3p remarkably suppressed cell migration in 143B and U2OS cells (n = 4). F-G. Overexpression of miR-766-3p inhibited cell invasion in 143B and U2OS lines (n = 4). Data are presented as the means ± SD. * P < 0.01.

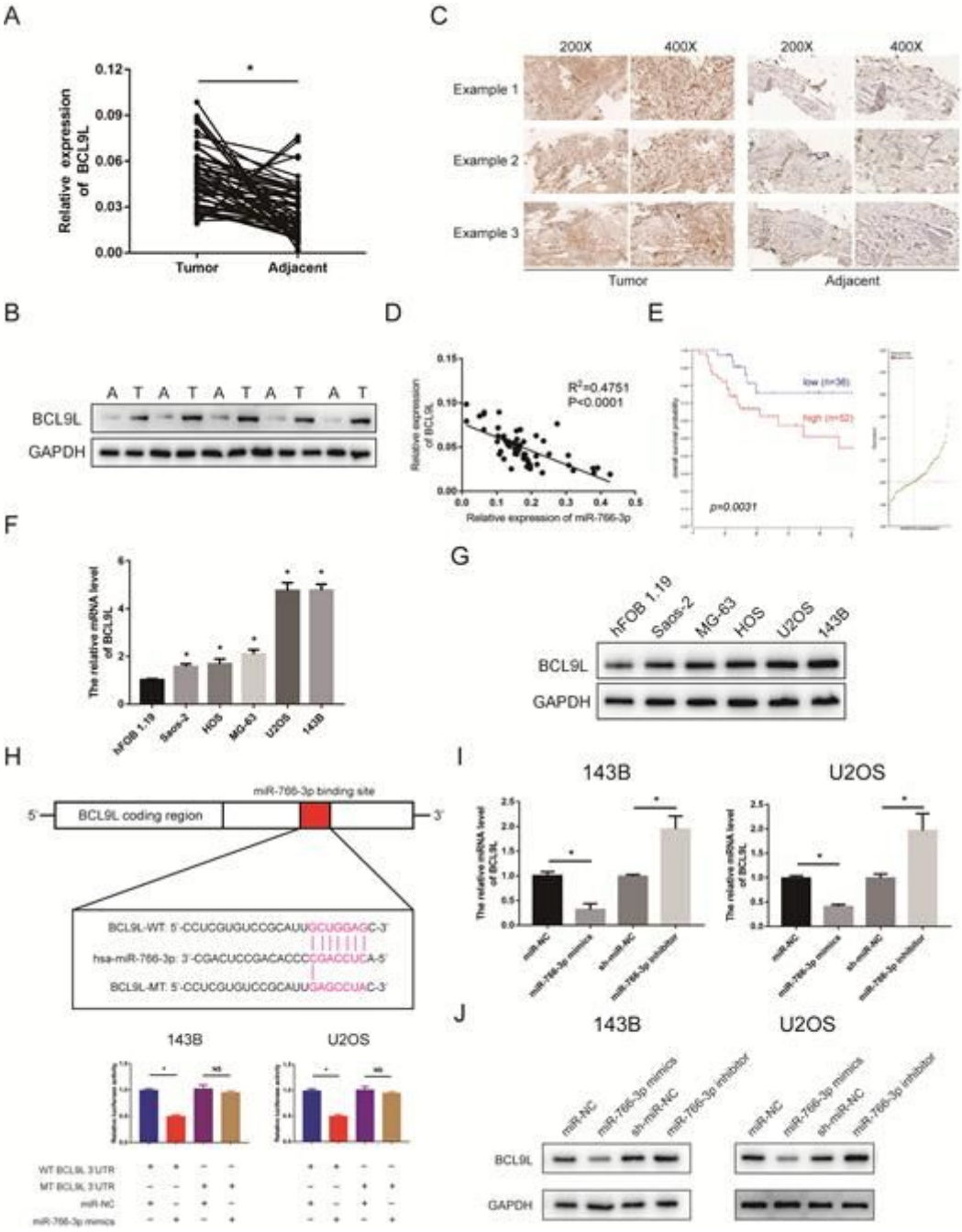

Figure 4

B-Cell Lymphoma 9-Like Protein (BCL9L) expression was upregulated in OS cell lines and tissues and was a target of miR-766-3p. A–C. BCL9L expression was remarkedly higher in OS tissues. D. Expression level of BCL9L was negatively correlated with miR-766-3p in OS tissues. E. Kaplan-Meier analysis demonstrated that patients with low BCL9L expression levels had a better prognosis according to an online database (https://hgserver1.amc.nl/cgi-bin/r2/main.cgi). F. The mRNA levels of BCL9Lwere upregulated in some OS cell lines, especially in MG63 and U2OS cells (n = 4). G. 143B and U2OS cells contained the most BCL9L protein compared to the other cell lines (n = 3). H. The WT-BCL9L-3'-UTR and MUT-BCL9L-3'-UTR were synthesized. Overexpressed miR-766-3p notably inhibited the luciferase activity of WT-BCL9L-3'-UTR but had no influence on MUT-BCL9L-3'-UTR in 143B and U2OS cells (n= 5). I. qRT-

PCR indicated that the BCL9L mRNA level was negatively regulated by miR-766-3p (n = 4). J. Western blotting supported that miR-766-3p negatively controls the expression level of BCL9L (n = 3). Data are presented as the means ± SD. * P < 0.01.

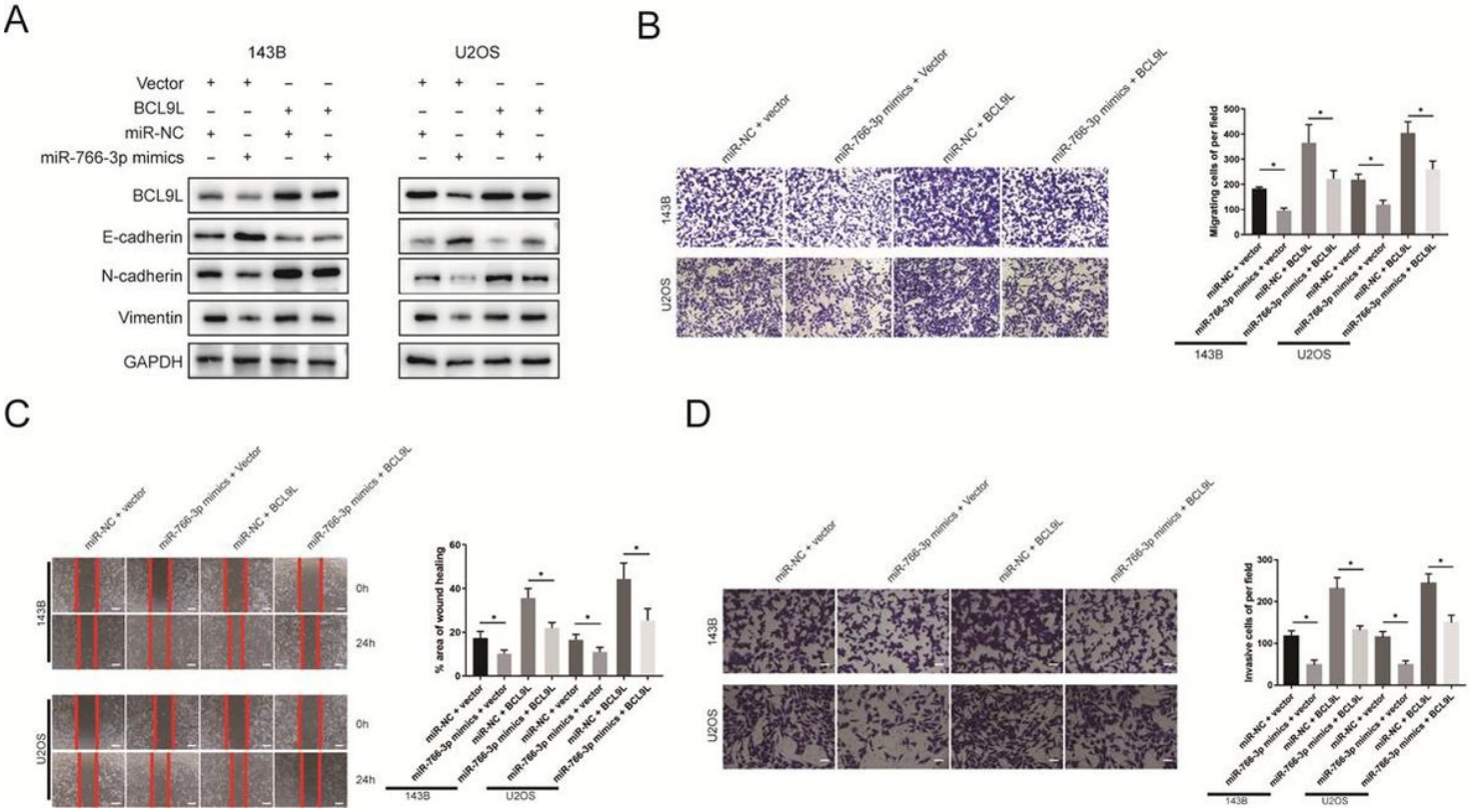

Figure 5

Upregulating BCL9L restored the effects of miR-766-3p mimics on OS cells. A. Western blotting showed that OS cells invasion and migration was remedied by overexpressed BCL9L (n = 3). B–C. BCL9L could reverse the augmented OS cell invasion and migration caused by miR-766-3p mimics (n = 4). D. These above results were confirmed by cell Transwell invasion assays (n = 4). Data are presented as the means ± SD. * P < 0.01.

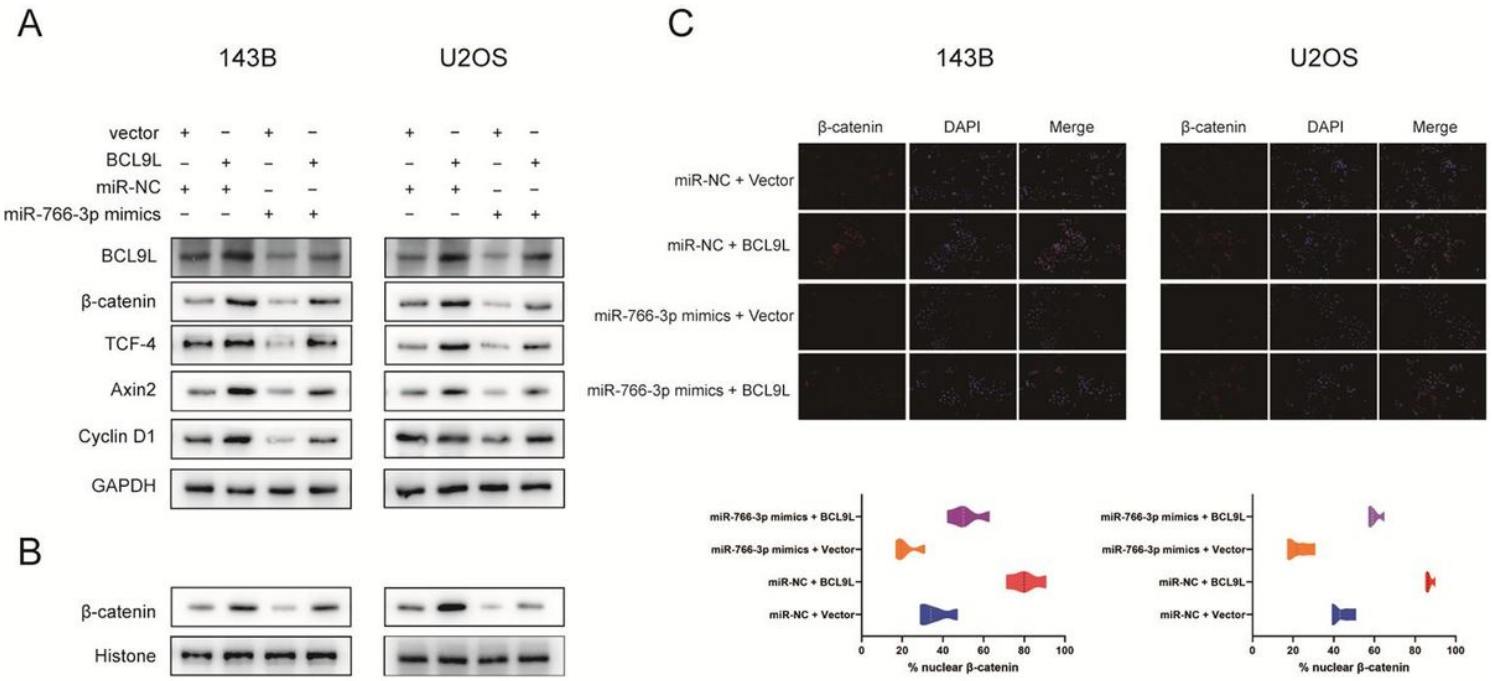

Figure 6

miR-766-3p regulated the β-catenin/TCF-4 signaling pathway via BCL9L. A. miR-766-3p mimics decreased the levels of BCL9L together with phosphorylation of β-catenin, TCF-4, Cyclin D1 and Axin2, but the suppressing effects were all remedied by overexpressed BCL9L (n = 3). B. The levels of β-catenin protein contained in nuclei had a negative correlation with the miR-766-3p expression and were positively correlated with the expression level of BCL9L (n = 3). C. miR-766-3p mimics enhanced β-catenin import into the nuclei of OS cells, and BCL9L could abolish this effect (n = 5). Data are presented as the means ± SD. * P < 0.01.

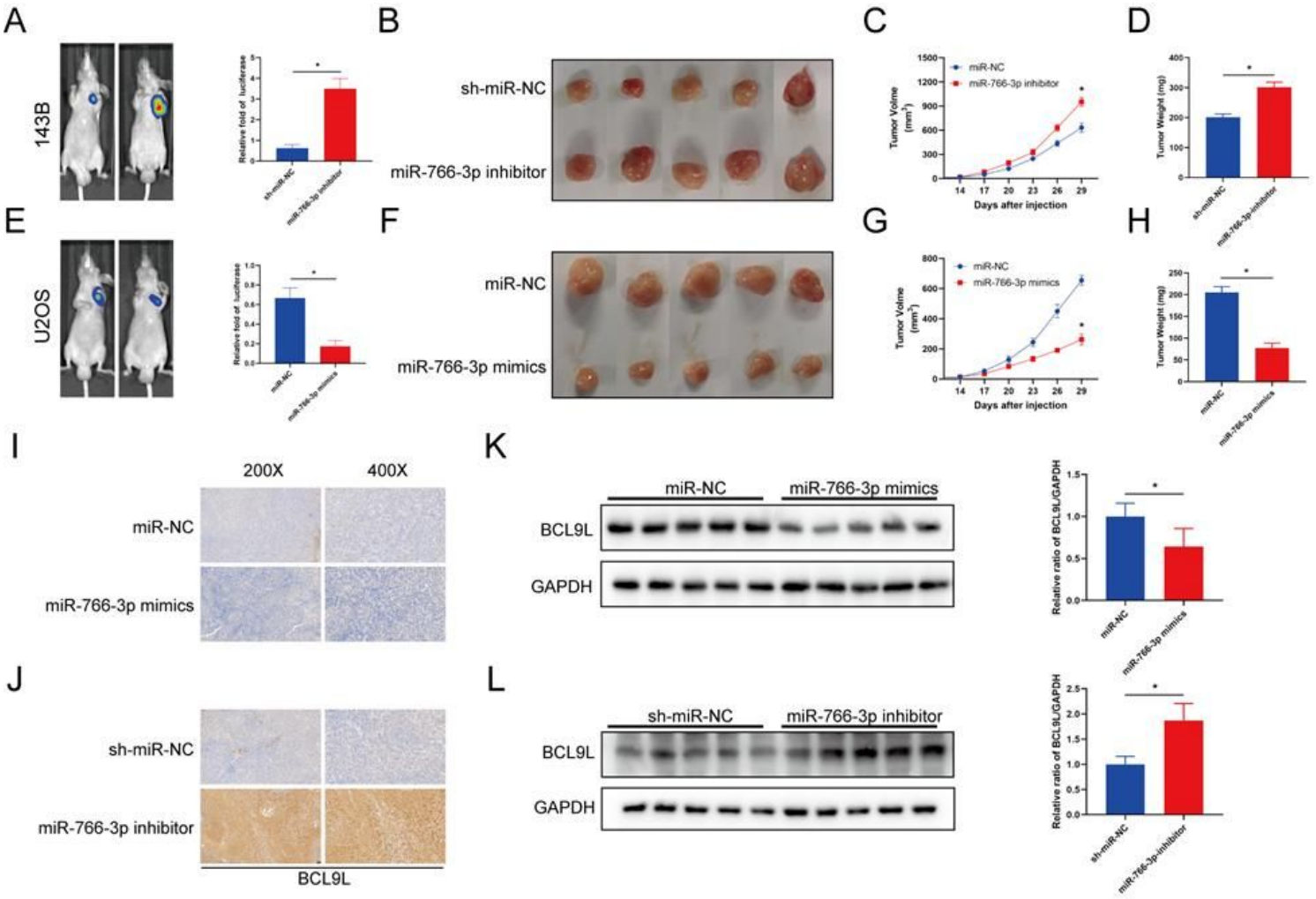

Figure 7

miR-766-3p suppressed xenograft tumor growth and pulmonary metastasis in vivo. A–D. Downregulation of miR-766-3p promoted the tumor growth of 143B cells, and tumor volume and average tumor weight were larger and heavier, respectively, than the sh-miR-NC group (n = 5). E–H. U2OS cells with high miR-766-3p expression significantly inhibited tumor growth in nude mice. The tumor volume was smaller and the average tumor weight was lighter in the miR-766-3p mimics group (n = 5). I–J. The immunohistochemistry assays showed that BCL9L expression was reduced in the miR-766-3p mimics group and enhanced BCL9L expression was observed in the miR-766-3p inhibitor group. K–L. Western blotting results confirmed that BCL9L expression was reduced in the miR-766-3p mimics group and enhanced in the miR-766-3p inhibitor group (n = 3). Data are presented as the means ± SD. * P < 0.01.

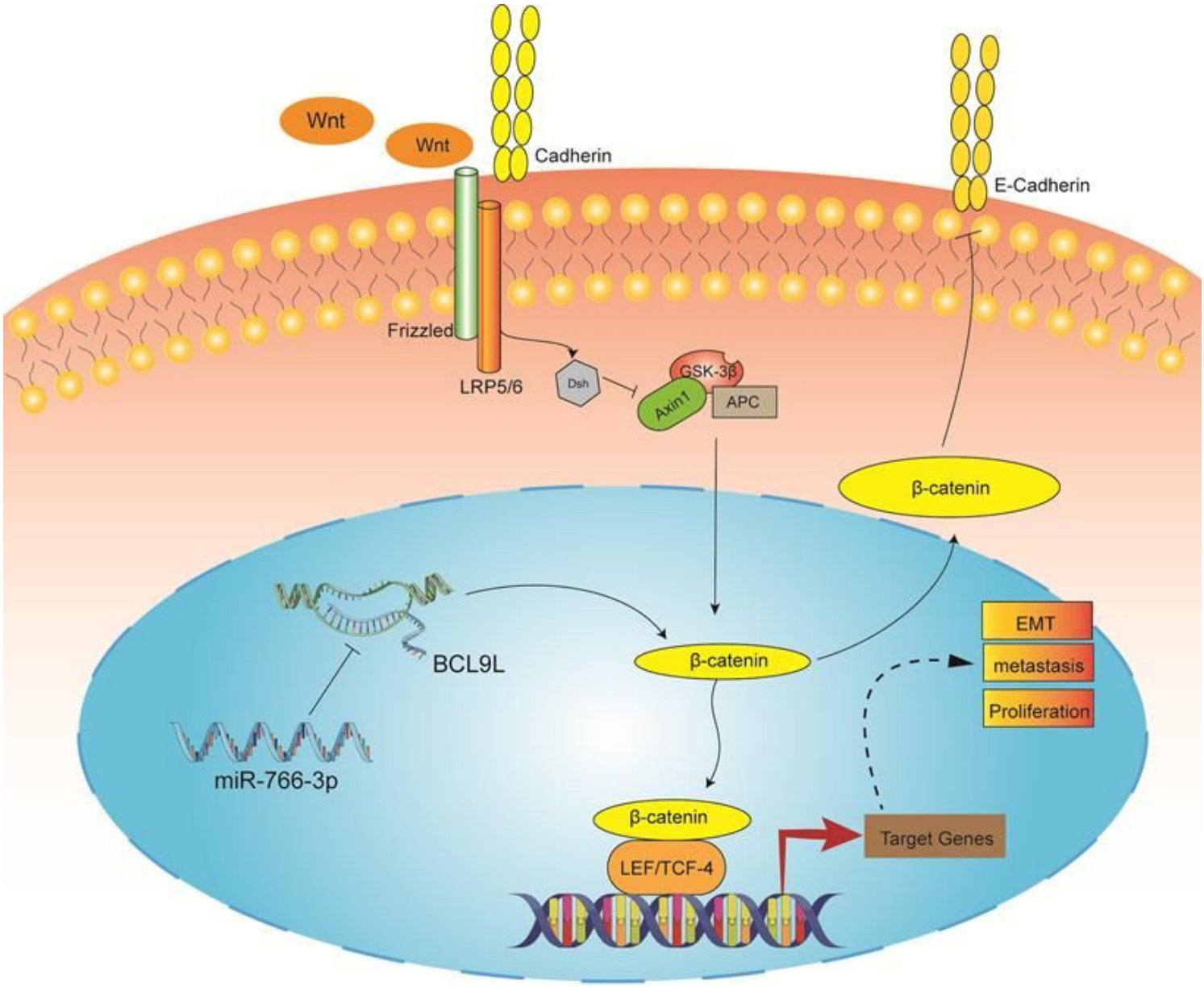

Figure 8

The molecular mechanism underlying the tumor-suppressive effect of miR-766-3p in OS. miR-766-3p targeting BCL9L inhibited proliferation, EMT, and metastasis by down-regulating β-catenin signaling pathway in OS cells.

Supplementary Files

This is a list of supplementary files associated with this preprint. Click to download.

- figureS3.tif
- figureS2.tif
- figureS1.tif
- tables1.pdf

- Supplementaryfiguresandtablelegends.docx